RSC Advances

PAPER

View Article Online
View Journal | View Issue

Cite this: *RSC Adv.*, 2022, **12**, 834

Green synthesis of novel 5-amino-bispyrazole-4-carbonitriles using a recyclable Fe_3O_4@SiO_2@vanillin@thioglycolic acid nano-catalyst†

Mohammad Nikpassand, *[a] Leila Zare Fekri, [b] Rajender S. Varma, [c] Lida Hassanzadi[a] and Farhad Sedighi Pashaki[a]

Bis(thioglycolic acid)-vanillin (2,2'-(((4-hydroxy-3-methoxyphenyl)methylene)bis(sulfanediyl))diacetic acid)-functionalized silica-coated Fe_3O_4 magnetic nanoparticles (Fe_3O_4@SiO_2@vanillin@thioglycolic acid MNPs) were synthesized and characterized by transmission electron microscopy (TEM), field emission scanning electron microscopy (FE-SEM), thermogravimetric analysis/differential thermogravimetry (TGA-DTG), X-ray powder diffraction (XRD), X-ray spectroscopy (EDX), vibrating sample magnetometry (VSM), zeta potential measurements and Fourier transform infrared spectroscopy (FT-IR). The ensuing MNPs offer an environmentally friendly procedure for the synthesis of novel 5-amino-pyrazole-4-carbonitriles *via* a three-component mechanochemical reaction of synthesized azo-linked aldehydes or synthesized pyrazolecarbaldehydes, malononitrile, and phenylhydrazine or *p*-tolylhydrazine adhering to the green chemistry principles; products were generated expeditiously in high yields. The catalyst could be quickly recovered and reused for six cycles with almost consistent activity. The structures of the synthesized 5-amino-pyrazole-4-carbonitrile compounds were confirmed by ^{1}H NMR, ^{13}C NMR, and FTIR spectra and elemental analyses. This new procedure has notable advantages such as operational simplicity, excellent yields, short reaction time, easy work-up, eco-friendliness and nontoxic catalyst. Also the catalyst can be easily recovered by an external magnetic field and reused for six consecutive reaction cycles without significant loss of activity.

Received 1st November 2021
Accepted 21st December 2021

DOI: 10.1039/d1ra08001f

rsc.li/rsc-advances

1. Introduction

One of the largest and most diverse groups of heterocyclic compounds are five-membered rings with more than one heteroatom and among them pyrazoles are 2-heteroatom heterocycles with aromatic stability. Pyrazoles and their salts have numerous biological and pharmaceutical properties such as anti-inflammatory, sedative, hypnotic, fever-resistant, anti-inflammatory, anti-fungal, antibacterial, anti-biotic and anti-tumor activity.[1,2] The synthesis of pyrazoles is specific because they are found in several different structures, such as pyrazoloisoquinolines and pyrazolopyrimidines, pyrazolopyridines and pyrazolo pyrazines.[3–6]

In recent years, the synthesis of pyrazoles has become pervasive as a large number of them have been prepared. Saleh *et al.* prepared the pyrazolo[3,4-*b*]pyridines from the reaction of phenylsulfone synthon with *N*-phenyl benzene carbohydrazonyl chloride with anti-inflammatory properties.[7] Trofimov *et al.* synthesized 3-amino-3-hydroxyalkyl-1-amino thiocarbonyl pyrazoles through the stereospecific cyclization reaction of 1,2-acetylene-3-hydroxynitriles with thiosemicarbazide,[7] Ortiz *et al.* prepared new series of pyrazoles during the Diels–Alder 1,2,3-triazoles reaction with diethyl acetylene dicarboxylate (DMAD) under pyrolysis of 3,4-dicarboxylate under solvent-free conditions.[8]

Recently, assorted methods have been proposed for the synthesis of diverse pyrazole derivatives.[9] These include the synthesis of 4-substituted pyrazoles *via* the reaction of 1,3-dipolar ring-forming of diazo compounds with triple bonds,[10] the three-component reaction among aromatic aldehydes, malononitrile and phenyl hydrazine,[11] the 2-methyl-3-nitrochrome starting material during the Michael addition reaction,[12] and the preparation of the oxoalkanenitrile or an aminonitrile derivatives, from a four-component reaction involving aryl aldehydes, hydrazines, ethylacetoacetate,

[a]*Department of Chemistry, Rasht Branch, Islamic Azad University, Rasht, Iran. E-mail: nikpassand@iaurasht.ac.ir*

[b]*Department of Chemistry, Payame Noor University, PO Box 19395-3697, Tehran, Iran. E-mail: chem_zare@yahoo.com; chem_zare@pnu.ac.ir*

[c]*Regional Centre of Advanced Technologies and Materials, Czech Advanced Technology and Research Institute, Palacký University in Olomouc, Šlechtitelů 27, 783 71 Olomouc, Czech Republic*

† Electronic supplementary information (ESI) available: General procedure and analytic data. See DOI: 10.1039/d1ra08001f

malononitrile,[13] and the reaction of enamines with hydroxylamine hydrochloride.[14]

The newer synthetic endeavours focus on the environmental aspects and the use greener techniques such as non-harmful solvents (such as water), solvent-free syntheses, inexpensive and abundant catalysts, one-step multicomponent reactions, among others where nanocatalysts play an important role in such green synthesis. Since the activity of the catalysts is related to the surface area of its particles, by reducing the size of the catalyst particles, the greater surface area will be exposed to the reactants, and with a small amount of catalyst the maximum efficiency can be achieved. Also, in the nano-catalysts, the attained selectivity leads to the prevention of the formation of undesirable products. Another characteristic of nanocatalysts is that they are heterogeneous besides being highly active, so they can be smoothly separated from the mixture at the end of the reaction.[14–18] Once the magnetic property is imparted to such nanocatalysts, it would be an ideal situation for their easy retrieval and reuse.

Herein, an efficient, green and simple method is presented for the preparation of pyrazolyl-5-amino-pyrazole-4-carbonitriles *via* mechanochemical means for the synthesis of new pyrazolyl-5-amino-pyrazole-4-carbonitrile or azo-linked 5-amino-pyrazole-4-carbonitriles with pre-formed pyrazolecarbaldehydes or azo-linked aldehydes, malononitrile, and phenylhydrazine at room temperature in the presence of a recyclable catalyst, bis(thioglycolic acid)-vanillin-functionalized silica-coated Fe_3O_4 nanoparticles (Fe_3O_4@SiO_2@Vanillin@Thioglycolic acid MNPs).

2. Results and discussion

In continuation of our work on the greener synthesis of organic molecules of interest,[19–29] and assorted literature in which magnetic nanoparticles have been used for multicomponent reactions,[30–33] the use of bis(thioglycolic acid)-vanillin-functionalized silica-coated Fe_3O_4 nanoparticles, (Fe_3O_4@SiO_2@vanillin@thioglycolic acid MNPs), is described as a new, reusable and effective catalyst for the synthesis of 5-amino-bispyrazole-4-carbonitrile derivatives and new azo-linked 5-amino-pyrazole-4-carbonitriles.

As shown in Scheme 1, the structure of Fe_3O_4@SiO_2@-vanillin@thioglycolic acid magnetic nanoparticle was realized in four steps from commercially available abundant materials. The Fe_3O_4@SiO_2 core–shell structures were sequentially treated with 3-chloropropyltrimethoxysilane followed by reaction with vanillin to obtain the vanillin-functionalized silica-coated Fe_3O_4 nanoparticles. In the final step, thioglycolic acid were added to the ensued product from earlier stage and Fe_3O_4@SiO_2@-vanillin@thioglycolic acid nanoparticles were produced with good efficiency and high purity (Scheme 1).

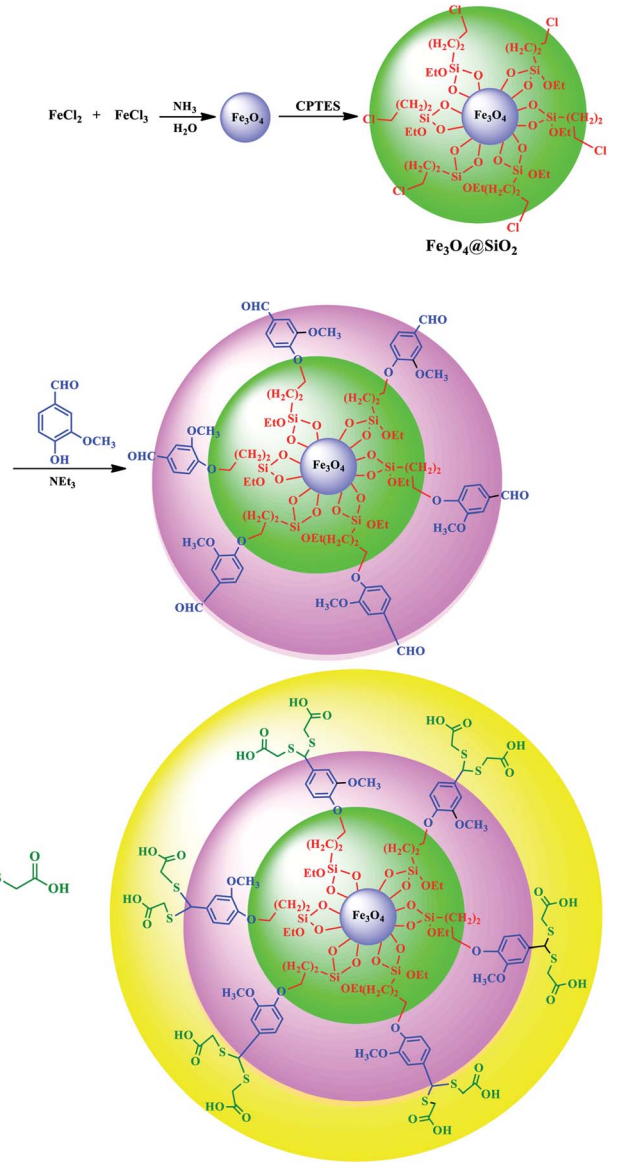

Scheme 1 The synthesis of Fe_3O_4@SiO_2@vanillin@thioglycolic acid MNPs.

2.1 Characterization of catalyst

Fig. 1 shows the FT-IR spectra of Fe_3O_4 MNPs, Fe_3O_4@SiO_2, Fe_3O_4@SiO_2@vanillin and Fe_3O_4@SiO_2@vanillin@thioglycolic acid MNPs which was conducted to identify the functional groups of the synthesized nanoparticles. In the spectra, the peaks at 3413 and 3433 cm^{-1} correspond to the hydrogen bonds in –OH stretching of Fe_3O_4@SiO_2@vanillin and –COOH group of thioglycolic acid in Fe_3O_4@SiO_2@vanillin@thioglycolic acid MNPs, respectively (Fig. 1c and d). The peaks at about 624–674 cm^{-1} correspond to the Fe–O bending (Fig. 1a–d), affirming the presence of Fe_3O_4 in the structure of these composites. The C=O stretching of vanillin carbonyl group of Fe_3O_4@SiO_2@-vanillin and Fe_3O_4@SiO_2@vanillin@thioglycolic acid are represented by the bands at 1692 and 1591 cm^{-1}, respectively, which are not visible in the FT-IR spectra of nanoparticles Fe_3O_4 and Fe_3O_4@SiO_2 (Fig. 1c and d). Also, the two peaks in the region ~910–1126 cm^{-1} belonging to Si–O–Si in SiO_2 shell appeared in Fig. 1b–d. The C–S bending at 674 cm^{-1} confirms

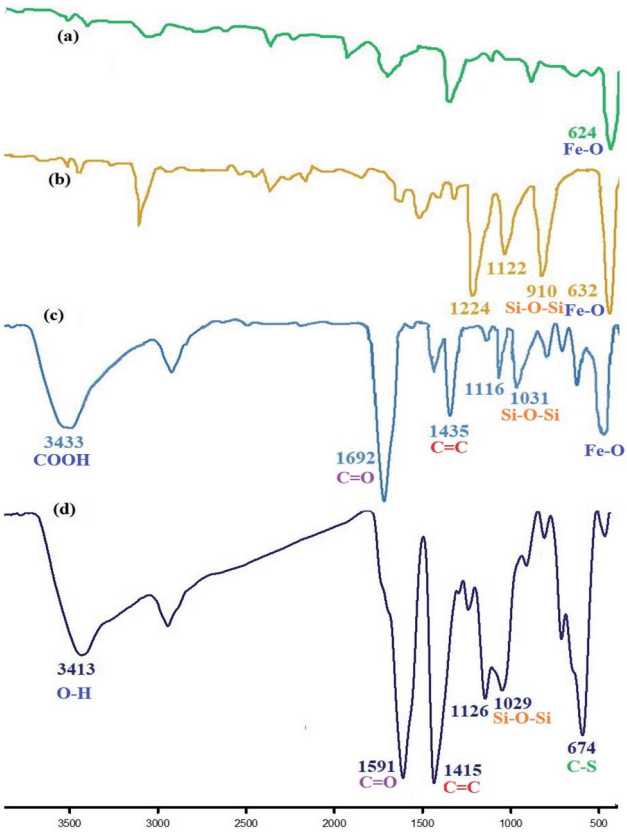

Fig. 1 The FT-IR spectra of (a) Fe_3O_4 MNPs; (b) Fe_3O_4@SiO_2; (c) Fe_3O_4@SiO_2@vanillin; (d) Fe_3O_4@SiO_2@vanillin@thioglycolic acid MNPs.

the presence of thioglycolic acid in the nanoparticle structure (Fig. 1d). The peaks at 1415 and 1435 cm^{-1}, respectively, in Fig. 1d and c corresponds to C=C stretching of vanillin carbonyl group of Fe_3O_4@SiO_2@vanillin and Fe_3O_4@SiO_2@-vanillin@thioglycolic acid.

The morphology and nanoparticle size of Fe_3O_4@SiO_2@-vanillin@thioglycolic acid nano-catalyst were determined and as shown in Fig. 2 and 3, TEM and FE-SEM images of the catalyst reveal that nanoparticles are formed with nearly

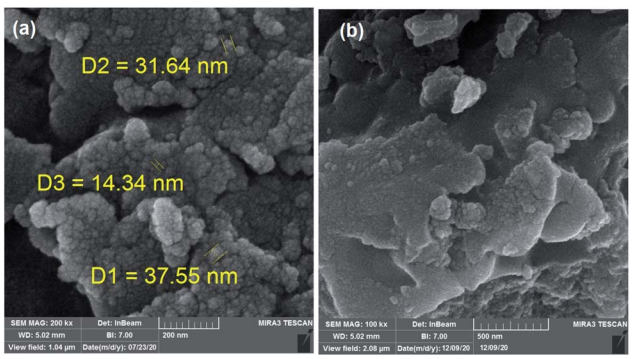

Fig. 2 The FE-SEM image of (a). Synthesized Fe_3O_4@SiO_2@-vanillin@thioglycolic acid MNPs; (b) after reusing for six times.

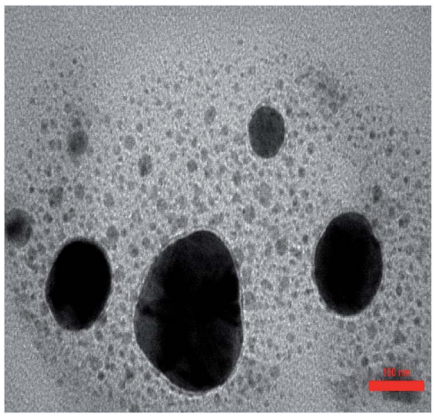

Fig. 3 The TEM image of synthesized Fe_3O_4@SiO_2@-vanillin@thioglycolic acid MNPs.

spherical morphology having a particle size of between 31 and 37 nm. Furthermore, TEM images show some aggregation, which reveals the successful grafting of the polymer on to magnetic nanoparticles.

To identify the elements of the composition of Fe_3O_4@-SiO_2@vanillin@thioglycolic acid MNPs, an energy dispersive X-ray spectroscopy (EDX) was obtained. The results of EDX analysis of the synthesized nanoparticle shows the existence of Fe (19.08 w/w, %), O (12.72 w/w, %), Si (0.74 w/w, %), S (9.53 w/w, %) and C (21.28 w/w, %) atoms in the structure thus confirming the presence of Fe_3O_4 core, SiO_2 and thioglycolic acid in the structure of Fe_3O_4@SiO_2@vanillin@thioglycolic acid MNPs (Fig. 4).

The vibrating sample magnetometer (VSM) plot of the Fe_3O_4@SiO_2@vanillin@thioglycolic acid MNPs is presented in Fig. 5. VSM measurements were carried out at room temperature by taking the solid sample on the tips of the vibrating rod and analysing in an applied magnetic field sweeping from −18 to 18 kOe (Fig. 5).

The X-ray diffraction (XRD) patterns for the catalyst in contrast to pure Fe_3O_4 confirms the formation of Fe_3O_4 MNPs. This pattern shows characteristic peaks at $2\theta = 24.1$, 30.2, 31.2, 35.8, 38.0, 48.8, 57.8 and 63.0. This position and relative intensities of all peaks are in a good agreement with standard

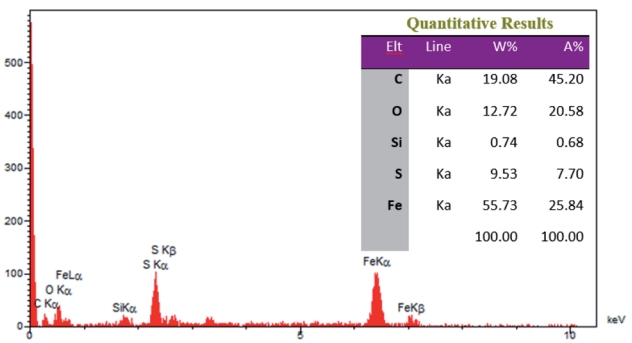

Fig. 4 The EDX image of synthesized Fe_3O_4@SiO_2@-vanillin@thioglycolic acid MNPs.

XRD pattern for the face-centred cubic structure of Fe_3O_4 and broad peak in 10–20° is related to SiO_2 (Fig. 6).

The thermal stability of the synthesized Fe_3O_4@SiO_2@-vanillin@thioglycolic acid catalyst was investigated by thermal gravimetric analysis (TGA) which helped to evaluate the stability of synthesized nanoparticles. TGA curve for the nanoparticles (Fig. 7) demonstrate 8% initial weight loss at temperatures lower than 100 °C and weight losses from 100–175 °C is related to evaporation of surface hydroxyl groups of the support. TGA analysis was used for determination of the weight changes of the organic functional groups of synthesized Fe_3O_4@SiO_2@-vanillin@thioglycolic acid upon heating; degradation of the organic groups was not observed in the range of 100 to 700 °C. Since the catalyst weight loss did not occur except above 600 °C implies its high thermal stability which is advantageous as many organic compounds may be synthesized at higher temperatures (Fig. 7).

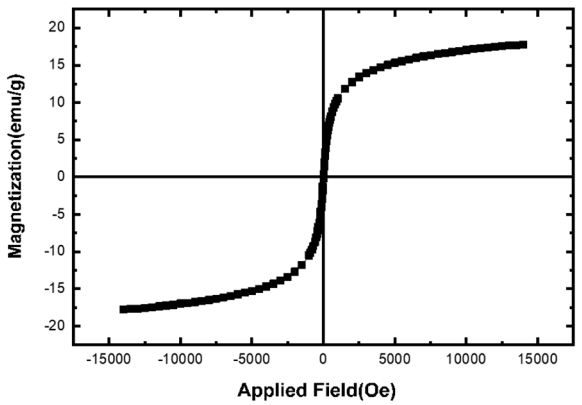

Fig. 5 The VSM image of synthesized Fe_3O_4@SiO_2@-vanillin@thioglycolic acid MNPs.

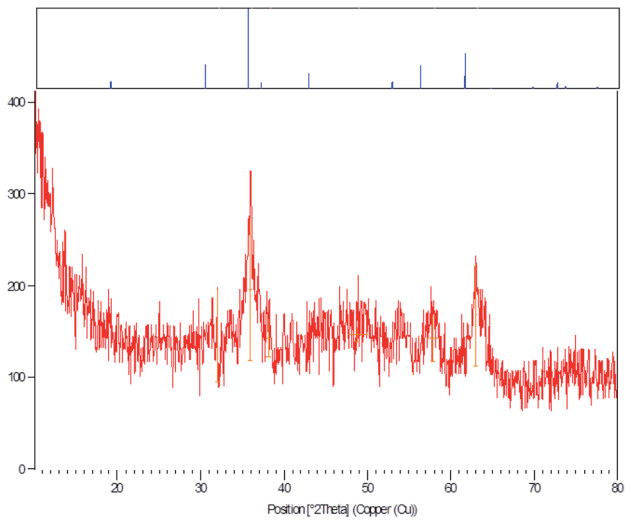

Fig. 6 The XRD image of synthesized Fe_3O_4@SiO_2@-vanillin@thioglycolic acid MNPs.

Zeta potential was used to understand the surface conditions of nanoparticles and predict their long-term dispersion stability. According to previous reports, nanoparticles with zeta potential values between +25 and −25 mV are usually very stable. As shown in Fig. 8, the zeta potential was scanned and the value of dispersed synthesized Fe_3O_4@SiO_2@vanillin@thioglycolic acid in deionized water, in absence of any electrolyte, was found to be −25.1 mV (Fig. 8).

2.2 Catalytic application

In order to evaluate the catalytic prowess of the synthesized heterogeneous catalyst, Fe_3O_4@SiO_2@vanillin@thioglycolic acid, in organic reactions, its activity was examined in an one-pot reaction by the grinding reaction between synthetized azo-linked aldehydes or pyrazolecarbaldehydes, malononitrile, and phenylhydrazine or *p*-tolyl hydrazine (Scheme 2).

Initially, 5-((4-chlorophenyl)diazenyl)-2-hydroxybenzaldehyde **1a** (1 mmol), malononitrile **2** (1 mmol), phenylhydrazine **3a**

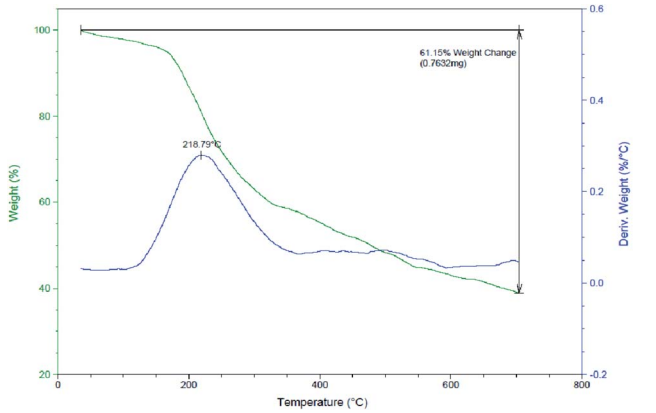

Fig. 7 The TGA-DTG image of synthesized Fe_3O_4@SiO_2@-vanillin@thioglycolic acid MNPs.

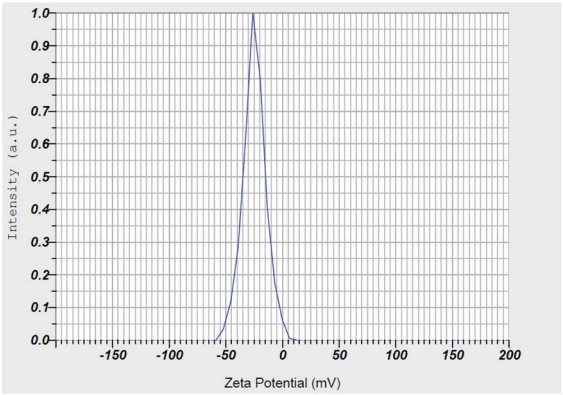

Fig. 8 The zeta potential image of synthesized Fe_3O_4@SiO_2@-vanillin@thioglycolic acid MNPs.

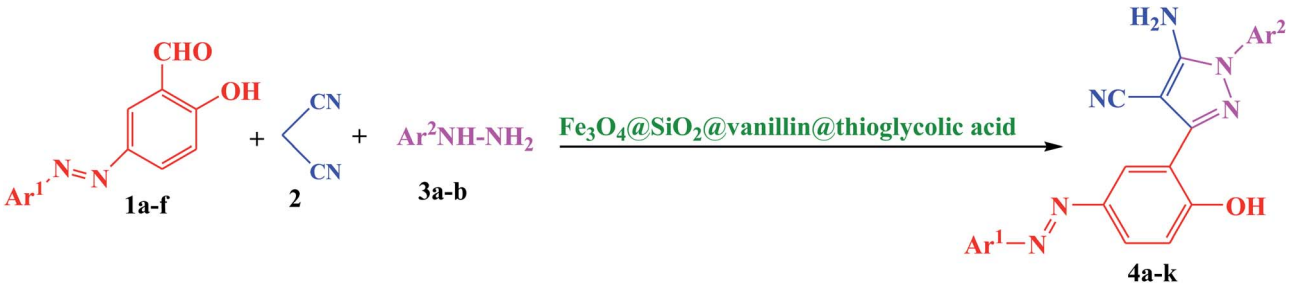

Scheme 2 Synthesis of novel azo-linked 5-amino-pyrazole-4-carbonitrile **4a–k** using of Fe_3O_4@SiO_2@vanillin@thioglycolic acid.

(1 mmol), in the presence of 0.1 g of available catalysts at 80 °C under different conditions was employed to produce 5-amino-3-(5-((4-chlorophenyl)diazenyl)-2-hydroxyphenyl)-1-phenyl-1*H*-pyrazole-4-carbonitrile (**4a**) and the effect of various factors such as the type of catalyst, its relative amount of raw material, reaction temperature, *etc.* on this sample reaction was investigated (Tables 1–3).

Table 1 Influence of catalyst types on reaction time and efficiency in synthesis of **4a**

Entry	Catalyst	Time (h)	Yield[a] (%)
1	—	24	55
2	Nano-SiO_2	6	63
3	K10	12	66
4	Nano-Fe_3O_4	6	72
5	Fe_3O_4@SiO_2@vanillin	6	78
6	Fe_3O_4@SiO_2@vanillin@thioglycolic acid	1.5	95
7[b]	[BBIM]Br	5	78
8[b]	[BBIM]HSO_4	5	83

[a] Reaction conditions: 5-((4-chlorophenyl)diazenyl)-2-hydroxybenzaldehyde **1a** (1 mmol), malononitrile **2** (1 mmol) and phenylhydrazine **3a** (1 mmol) was used under solvent free condition. [b] 2 mL of ionic liquid were used for ionic liquids in entries 7 and 8.

Table 2 Effect of temperature on synthesis of **4a** using of Fe_3O_4@SiO_2@vanillin@thioglycolic acid

Entry	Temperature (°C)	Time (h)	Yield (%)
1	25	1.5	95
2	60	1.5	90
3	80	1.5	94

Table 3 Investigation of the amount of catalyst used in the synthesis of **4a**

Entry	Amount of catalyst (g)	Time (h)	Yield (%)
1	0.05	5	80
2	0.1	1.5	95
3	0.2	1.5	95

In the synthesis of **4a**, the reaction of 5-((4-chlorophenyl) diazenyl)-2-hydroxybenzaldehyde **1a** (1 mmol), malononitrile **2** (1 mmol) and phenylhydrazine **3a** (1 mmol) and 0.1 g of Fe_3O_4@SiO_2@vanillin@thioglycolic acid was used and the reaction was carried out at varying temperatures 25, 60 and 80 °C; optimum temperature for this reaction was found to be room temperature (25 °C) (Table 2).

Synthesis of product **4a** with varying amounts of Fe_3O_4@SiO_2@vanillin@thioglycolic acid at room temperature was investigated and it was found that using of 0.1 g of the desired catalyst per 1 mmol of primary reaction aldehyde afforded better yield in shorter time period (Table 3).

To establish the efficiency and general scope of the mechanochemical reaction, various azo-linked aldehydes, malononitrile, and phenylhydrazine or *p*-tolyl hydrazine were reacted in the presence of Fe_3O_4@SiO_2@vanillin@thioglycolic acid at room temperature (Scheme 2 and Table 4).

In order to expand the scope of the reaction, synthesized pyrazolecarbaldehydes including a range of electron-releasing or electron-withdrawing groups were also examined (Table 5); as presented in Table 5 both electron-donating and electron-withdrawing groups lead to the corresponding products in excellent yields.

Additionally, various synthetized pyrazole carbaldehydes, malononitrile, and phenylhydrazine were reacted in the presence of Fe_3O_4@SiO_2@vanillin@thioglycolic acid at room temperature (Scheme 3 and Table 5).

The proposed mechanism for the synthesis of novel 5-amino-pyrazole-4-carbonitriles using of Fe_3O_4@SiO_2@vanillin@thioglycolic acid MNPs is presented in Scheme 3. Initially, Fe_3O_4@SiO_2@Vanillin@Thioglycolic acid nanocatalyst seems to activate the synthesis of synthetic aldehyde by protonation of the carbonyl functional group. Then, malononitrile performs Knoevenagel condensation with intermediate **2** and intermediate **8** is obtained. Next, the Michael addition of phenylhydrazine, followed by cyclization and intermediate **11** is produced. Finally, enol–keto rearrangement, dehydration, and the separation of the nanocatalyst, generated the desired product **13** (Scheme 4).

The recyclability and reusability of catalyst was studied in the model one-pot grinding reaction between various azo-linked aldehydes, diverse hydrazines and malononitrile. At the end

Table 4 Synthesis of azo-linked 5-amino-pyrazole-4-carbonitriles **4a–k** using of Fe_3O_4@SiO_2@vanillin@thioglycolic acid

Entry	Product	Structure	Time (min)	Yield[a,b] (%)
1	**4a**	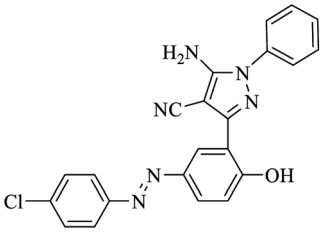	90	95
2	**4b**	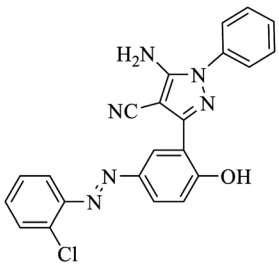	90	92
3	**4c**	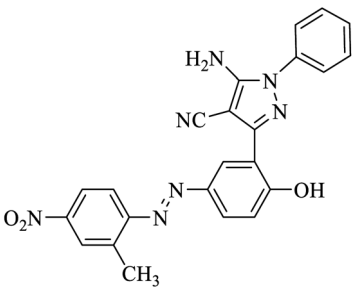	120	92
4	**4d**	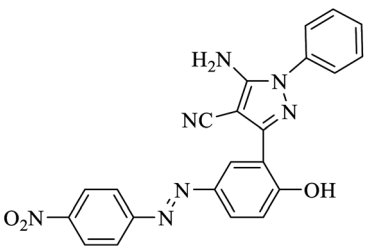	90	95
5	**4e**	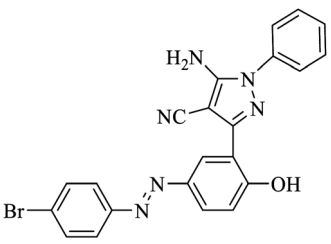	90	94
6	**4f**	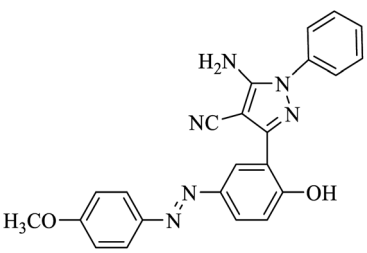	150	91

Table 4 (*Contd.*)

Entry	Product	Structure	Time (min)	Yield[a,b] (%)
7	**4g**	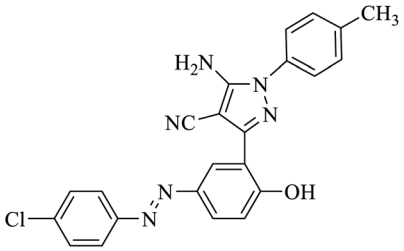	90	92
8	**4h**	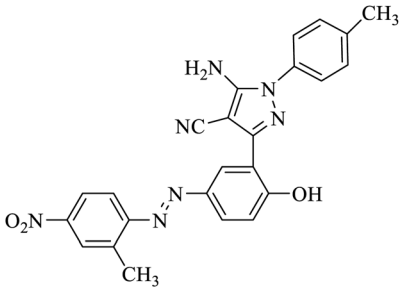	120	91
9	**4i**	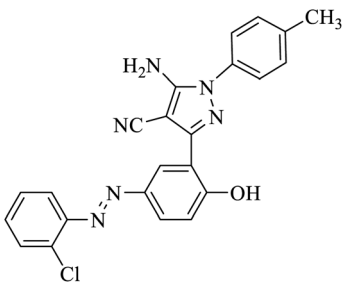	120	90
10	**4j**	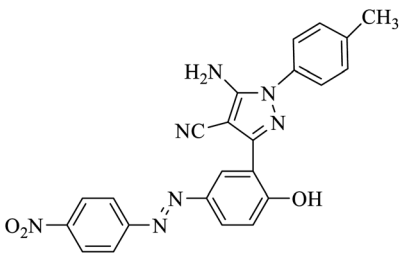	90	96
11	**4k**	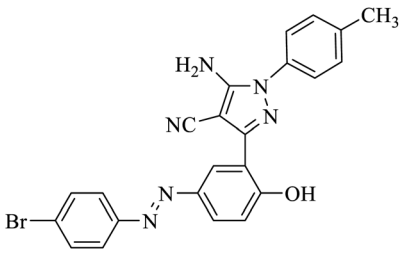	90	95

[a] Yields based upon the starting azo-linked aldehydes. [b] A mixture of synthesized azo-linked salicylaldehyde (1 mmol), various hydrazines (1 mmol), malononitrile (1 mmol), and Fe_3O_4@SiO_2@vanillin@thioglycolic acid (0.1 g) were mixed at room temperature for the required reaction time.

of the reaction, the separated catalyst could be reused after being washed with warm EtOH and drying at 80 °C; Fe_3O_4@-SiO_2@vanillin@thioglycolic acid MNPs was reused again for subsequent experiments under similar reaction conditions without any noticeable loss of its activity; yields of the product decreased only slightly after reusing the catalyst for six times (Table 6).

Table 5 Synthesis of 5-amino-bispyrazole-4-carbonitriles **6a–j** using of Fe_3O_4@SiO_2@vanillin@thioglycolic acid

Entry	Product	Structure	Time (min)	Yield[a,b] (%)
1	**6a**	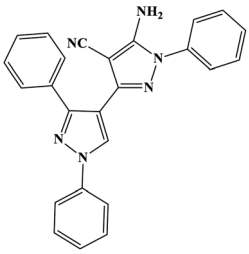	120	92
2	**6b**	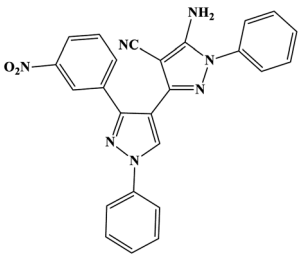	90	94
3	**6c**	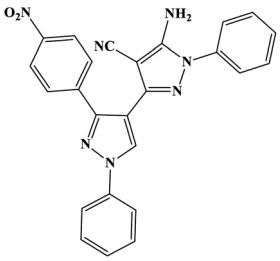	90	95
4	**6d**	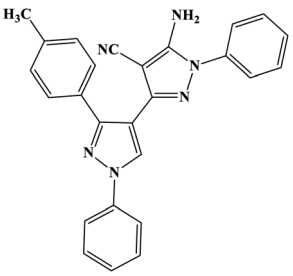	120	92
5	**6e**	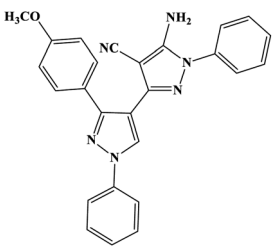	120	91
6	**6f**	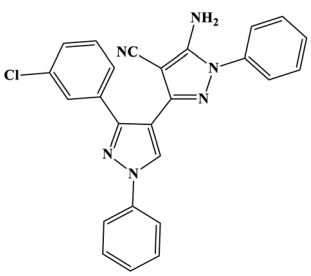	90	93

Table 5 (*Contd.*)

Entry	Product	Structure	Time (min)	Yield[a,b] (%)
7	**6g**	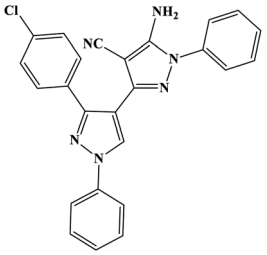	90	95
8	**6h**	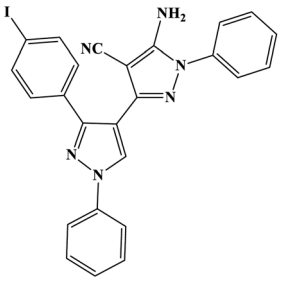	90	95
9	**6i**	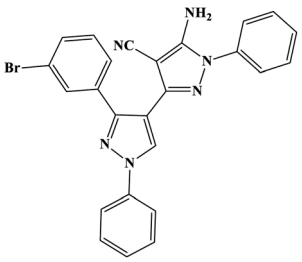	90	92
10	**6j**	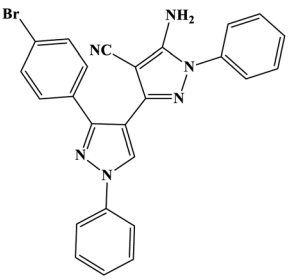	90	93

[a] Yields based upon the starting synthetized pyrazole carbaldehydes. [b] A mixture of synthetized pyrazolecarbaldehyde (1 mmol), various hydrazines (1 mmol), malononitrile (1 mmol) and Fe_3O_4@SiO_2@vanillin@thioglycolic acid (0.1 g) were mixed at room temperature for the required reaction time.

Scheme 3 Synthesis of novel 5-amino-bispyrazole-4-carbonitrile **6a–j** using of Fe_3O_4@SiO_2@vanillin@thioglycolic acid.

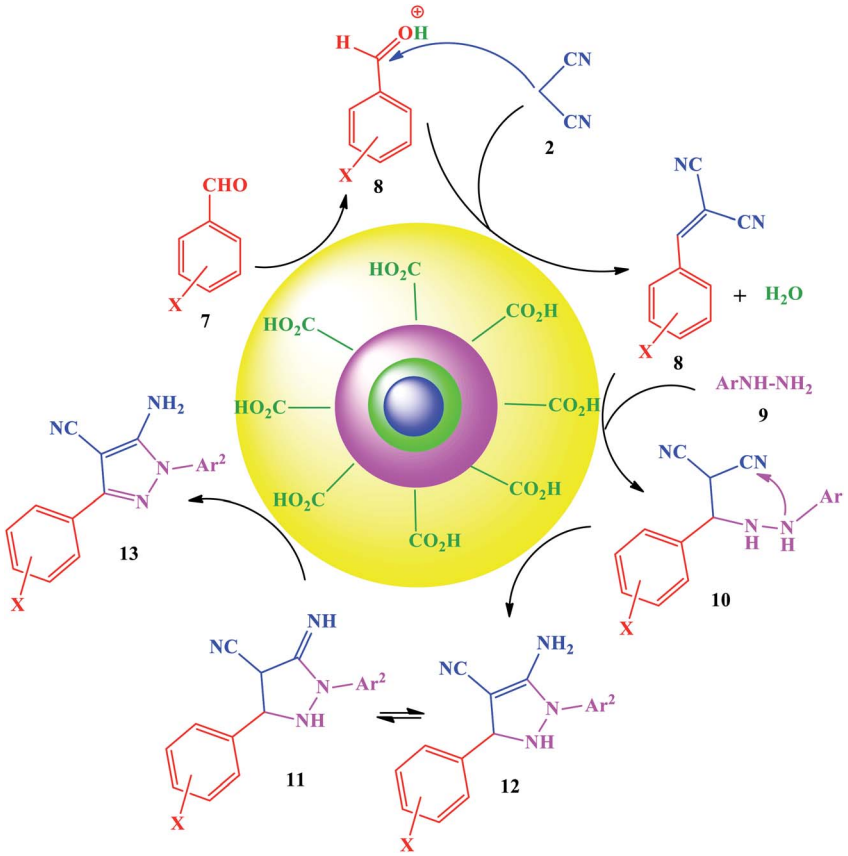

Scheme 4 The suggested mechanism for the synthesis of novel 5-amino-pyrazole-4-carbonitriles using of Fe_3O_4@SiO_2@vanillin@thioglycolic acid MNPs.

Table 6 Reusability of catalyst in the synthesis of **6a**

Run	1	2	3	4	5	6	7
Yield	92	92	92	91	91	92	85
Mp (°C)	134–136	135–137	134–136	135–137	133–135	134–136	133–135

3. Conclusion

In conclusion, we have designed Fe_3O_4@SiO_2@-vanillin@thioglycolic acid MNPs as a new, eco-friendly, inexpensive, mild and reusable catalyst for the mechanochemical synthesis of azo-linked 5-amino-pyrazole-4-carbonitriles and 5-amino-bispyrazole-4-carbonitriles under solvent-free conditions. High yields, a simple work-up procedure, adherence to the basic principles of green chemistry, environmentally friendly nature and deployment of readily available abundant ingredients, ease of separation and recyclability of the magnetic catalyst and waste reduction are some of the advantages of this method.

Conflicts of interest

There are no conflicts to declare.

Acknowledgements

Financial support from the Research Council of Rasht Branch, Islamic Azad University, Rasht, Iran is sincerely acknowledged.

References

1 X. H. Liu, P. Cui, B. A. Song, P. S. Bhadury, H. L. Zhu and S. F. Wang, *Bioorg. Med. Chem.*, 2008, **16**, 4075.
2 A. Bekhite and T. A. Aziem, *Bioorg. Med. Chem.*, 2004, **12**, 1935.
3 F. Karci and A. Demircah, *Dyes Pigm.*, 2008, **76**, 97.
4 Y. C. Wu, Y. J. Chen, H. J. Li, X. M. Zou, F. Z. Hu and H. Z. Yang, *J. Fluorine Chem.*, 2006, **127**, 409.
5 T. I. El-Emary, *J. Chin. Chem. Soc.*, 2006, **53**, 391.
6 T. S. Saleh and N. M. A. El-Rahman, *Ultrason. Sonochem.*, 2009, **16**, 237.

7 B. A. Trofimov, A. G. Malkina, A. P. Borisova, V. V. Nosyreva, O. A. Shemyakina, O. N. Kazheva, G. V. Shilov and O. A. Dyachenko, *Tetrahedron Lett.*, 2008, **49**, 3104.
8 A. D. Ortiz, A. D. Cozar, P. Prieto, A. D. L. Hoz and A. Moreno, *Tetrahedron Lett.*, 2006, **47**, 8761.
9 A. M. Salaheldin, A. M. F. Oliveira-Campos and L. M. Rodrigues, *Tetrahedron Lett.*, 2007, **48**, 8819.
10 R. Martin, M. R. Rivero and S. L. Buchwald, *Angew. Chem., Int. Ed. Engl.*, 2006, **45**, 7079.
11 P. S. Bhale, B. Sakharam and U. B. Chanshetti, *Res. J. Chem. Sci.*, 2014, **4**, 16.
12 K. Takagi, M. Tanka, Y. Murakami, K. Ogura, K. Ishii, H. Morita and T. Aotsuka, *J. Heterocycl. Chem.*, 1987, 1003.
13 H. Kiyani, H. A. Samimi, F. Ghorbani and S. Esmaieli, *Curr. Chem. Lett.*, 2013, **2**, 197.
14 Y. Tominaga, Y. Matsuoka, Y. Oniyama, H. Komiya, Y. Uchimura, M. Hirayama and S. Kohra, *J. Heterocycl. Chem.*, 1990, **27**, 647.
15 E. B. Towne, W. H. Moore and J. B. Dickey, *US Pat.*, 3.336.285, 15.8.1967, (Eastman Kodak Co.), *Chem. Abstr.*, 1968, **68**, 14072r.
16 S. T. Fardood, A. Ramazani and S. Moradi, *J. Sol-Gel Sci. Technol.*, 2017, **82**, 432.
17 V. Polshettiwar and R. S. Varma, *Green Chem.*, 2010, **12**, 743.
18 H. Kiyani and M. Bamdad, *Res. Chem. Intermed.*, 2018, **44**, 2761.
19 Z. Pourkarim and M. Nikpassand, *J. Mol. Struct.*, 2020, 128433.
20 M. Nikpassand, L. Zare Fekri, L. Karimian and M. Rassa, *Curr. Org. Synth.*, 2015, **12**, 358.
21 A. Masoumi Shahi, M. Nikpassand and L. Zare Fekri, *Org. Prep. Proced. Int.*, 2019, **51**, 521.
22 L. Zare Fekri, M. Nikpassand and S. Nazari Khakshoor, *J. Organomet. Chem.*, 2019, **894**, 18.
23 M. Nikpassand, L. Zare Fekri and S. Sanagou, *Dyes Pigm.*, 2017, **136**, 140.
24 A. Masoumi Shahi, M. Nikpassand, H. Fallah-Bagher-Shaidaei and L. Zare Fekri, *Polycyclic Aromat. Compd.*, 2020, **40**, 1143.
25 M. Nikpassand, L. Zare Fekri and A. Pourahmad, *J. CO2 Util.*, 2018, **27**, 320.
26 M. Nikpassand, *Dyes Pigm.*, 2020, **173**, 107936.
27 M. Nikpassand, L. Zare Fekri and P. Farokhian, *Ultrason. Sonochem.*, 2016, **28**, 341.
28 M. Nikpassand and D. Pirdelzendeh, *Dyes Pigm.*, 2016, **130**, 314.
29 B. Aghazadeh and M. Nikpassand, *Carbohydr. Res.*, 2019, **483**, 107755.
30 H. T. Nguyen, N. P. T. Le, D. K. N. Chaua and P. H. Tran, *RSC Adv.*, 2018, **8**, 35681.
31 H. T. Nguyen, N. P. T. Le, D. K. N. Chaua and P. H. Tran, *RSC Adv.*, 2019, **9**, 38148.
32 H. T. Nguyen, V. A. Truong and P. H. Tran, *RSC Adv.*, 2020, **10**, 25358.
33 H. T. Nguyen and P. H. Tran, *RSC Adv.*, 2020, **10**, 9663.